REDUCED-ORDER MODELING FOR ABLOWITZ-LADIK EQUATION

Murat Uzunca
Department of Mathematics, Sinop University
Sinop-Turkey
muzunca@sinop.edu.tr

Bülent Karasözen
Institute of Applied Mathematics & Department of Mathematics
Middle East Technical University
Ankara-Turkey
bulent@metu.edu.tr

ABSTRACT

In this paper, reduced-order models (ROMs) are constructed for the Ablowitz-Ladik equation (ALE), an integrable semi-discretization of the nonlinear Schrödinger equation (NLSE) with and without damping. Both ALEs are non-canonical conservative and dissipative Hamiltonian systems with the Poisson matrix, depending quadratically on the state variables and with quadratic Hamiltonian. The full-order solutions are obtained with the energy preserving midpoint rule for the conservative ALE and exponential midpoint rule for the dissipative ALE. The reduced-order solutions are constructed intrusively by preserving the skew-symmetric structure of the reduced non-canonical Hamiltonian system by applying proper orthogonal decomposition with the Galerkin projection. For an efficient offline-online decomposition of the ROMs, the quadratic nonlinear terms of the Poisson matrix are approximated by the discrete empirical interpolation method. The computation of the reduced-order solutions is further accelerated by the use of tensor techniques. Preservation of the Hamiltonian and momentum for the conservative ALE, and preservation of dissipation properties of the dissipative ALE, guarantee the long-term stability of soliton solutions.

Keywords Hamiltonian systems, nonlinear Schrödinger equation, proper orthogonal decomposition, discrete empirical interpolation, tensors
MR2000 Subject Classification: 65M06; 65P10; 37J05; 37M15; 76B15

1 Introduction

The nonlinear Schrödinger equation (NLSE) is used frequently for modeling wave propagation phenomena in different areas of physics, chemistry, and engineering. It is one of the most important models of mathematical physics, with application to different fields such as plasma physics, nonlinear optics, water waves, bi-molecular dynamics, and many other fields. Ablowitz-Ladik equation (ALE) [1] represents an integrable discretization of NLSE [24, 36, 38]. There are two classes of geometric integrators for Hamiltonian systems; symplectic and energy preserving integrators. Unfortunately, it is not possible, in general, to preserve both energy and the symplectic form at the same time. The ALE is a non-canonical Hamiltonian system with a state-dependent Poisson structure, so that the symplectic integrators are not applicable. Therefore, the ALE is integrated in time with the energy preserving discrete gradient methods. The average vector field (AVF) method and the mid-point rule exactly preserve the energy (Hamiltonian) and the quadratic invariants such as the momentum and norm of the ALE [16]. The linearly damped NLSE and the associated damped ALE are linearly perturbed non-canonical Hamiltonian systems, i.e., conservative systems with added linear damping. Discrete gradient methods have been also used in dissipative settings. In order to preserve the dissipation of energy, momentum, and norm with the correct rate, the damped ALE is integrated in time with exponential mid-point rule [30].

Model order reduction (MOR) allows to construct low-dimensional reduced-order models (ROMs) for the high dimensional full-order models (FOMs). The full-order solutions are projected on low dimensional reduced spaces with the proper orthogonal decomposition (POD) [8, 37], which is a widely used ROM technique. Applying the POD with the Galerkin projection, the dominant POD modes are extracted from the snapshots of the full-order solutions. We refer to the recent book [7] for an overview of the available MOR techniques. Conservation of nonlinear invariants like the energy is not, in general, guaranteed with conventional ROM. The violation of such invariants often results in a qualitatively wrong or unstable reduced system, even when the high-fidelity system is stable. It is well known that conservation law plays an important role in conservative PDEs such as the NLSE with quasi-periodic solutions and solitons. The stability of the ROMs over long-time integration has been investigated in the context of Lagrangian systems [13], and for port-Hamiltonian systems [14]. For canonical Hamiltonian systems, like the linear wave equation, Sine-Gordon equation, NLSE, singular value decomposition (SVD) based symplectic model reduction techniques with POD Galerkin projection are constructed with orthogonal [35], and non-orthogonal bases [10] capturing the symplectic structure of Hamiltonian systems in order to ensure long term stability of the reduced model. For parametric Hamiltonian systems, symplectic bases are generated using greedy approaches in [3, 12]. Parallel to these, energy (Hamiltonian) preserving ROMs have been developed for non-canonical Hamiltonian PDEs like the Korteweg-de Vries (KdV) equation [20, 29, 39] and NLSE [25], and with state-dependent Poisson structure such as rotating shallow water equations [26, 27]. These are all global ROM techniques, that maintain the globalized properties such as the symplectic structure or the Hamiltonian of the full order data in the reduced order representation do not possess a global low-rank structure. These approaches can provide robust and efficient reduced models, but they require a sufficiently large approximation space to achieve accurate solutions. This is due the fact that in Hamiltonian PDEs, non-dissipative phenomena do not possess a global low-rank structure. Hence, local reduced spaces seem to be more effective for this systems. Recently, localized ROM have been developed for Hamiltonian PDEs, which are more effective than the global POD based ROMs. A reduced basis method is developed in [22] for non-canonical Hamiltonian systems that preserves general Poisson structure by "freezing" the phase space manifold structure in each discrete temporal interval, then recasts the local problem in canonical form. In this way, a local reduced model is constructed in canonical Hamiltonian form. In [23], a rank-adaptive structure-preserving dynamical reduced-based method is constructed relying on a residual error estimator. The FOM is approximated on local reduced spaces that are adapted in time using dynamical low-rank approximation techniques. In [32], nonlinear structure-preserving model reduction is proposed where the reduced phase space evolves in time. The reduced system is obtained by a symplectic projection of the Hamiltonian vector field onto the tangent space of the approximation manifold at each reduced state as in dynamical low-rank approximation. Also for dissipative Hamiltonian systems, structure-preserving ROMs have been developed in [2, 34]. We refer to [21] for an overview about the structure-preserving ROMs for Hamiltonian systems.

In this paper, we develop ROMs for the conservative and damped ALEs while preserving its physical properties like conservation/dissipation of the Hamiltonian and the momentum which is a quadratic invariant. We construct energy preserving ROMs for conservative ALE with state-dependent Poisson matrix following the approach in [20, 29] where the authors construct an energy preserving ROM for the KdV equation in non-canonical Hamiltonian form with constant skew-symmetric matrix and by the AVF or mid-point method. Following the same approach with an additional linear damping term, a ROM is constructed that preserves the dissipation of the energy and the momentum of the dissipative ALE. An important feature of the ROMs is the offline-online decomposition. The computation of the FOM and the construction of the POD basis are performed in the offline stage, whereas the reduced system is solved by projecting the problem onto the low-dimensional reduced space in the online stage. The nonlinear term in the Poisson matrix is approximated with the hyper-reduction technique, i.e., discrete empirical interpolation method (DEIM) [15, 17], so that offline and online stages are separated. For dynamical systems such as the ALEs with wave-type solutions, a relatively large number of POD modes are needed to represent the physical behavior of the system in reduced-order form. Therefore, the reduced-order system should be solved efficiently. Here, the quadratic reduced system is solved utilizing tensor techniques [5, 6, 26] by the use of MULTIPROD [28] in order to speed up online computations.

Construction of the efficient structure-preserving ROM for non-canonical Hamiltonian systems with a state-dependent Poisson matrix, such as the conservative and dissipative ALEs, is challenging. The main contributions of the paper can be summarized below:

- Considering the conservative ALE equation in skew-gradient form and applying the energy preserving mid-point method, the reduced Hamiltonian and momentum are preserved, which guarantees the long-term stability of the solutions.

- Dissipation of the reduced Hamiltonian and momentum of the linearly perturbed ALE is preserved with the correct rate by the ROMs by integrating in time with the exponential mid-point method.

- Approximation of the nonlinear terms with DEIM enables offline-online decomposition. The solutions of the resulting linear-quadratic system are accelerated by applying tensor techniques.
- The soliton solutions of the conservative and dissipative ALEs are captured accurately by the ROMs in long time integration.

The paper is organized as follows. In Section 2, the high fidelity discretization that preserves the conservation/dissipation property of the conservative/damped ALEs is presented. In Section 3, the structure-preserving ROMs with POD and DEIM are described. Two numerical tests in Section 4 demonstrate the structure-preserving properties of the ROMs. The paper ends with some conclusions in Section 5.

2 Discretization of the conservative and dissipative Ablowitz-Ladik equations

The NLSE is a well-known nonlinear partial differential equation (PDE) with a broad spectrum of applications, ranging from wave propagation in nonlinear media to nonlinear optics, molecular biology, quantum physics, quantum chemistry, and plasma physics. We consider the NLSE described by

$$i\dot{\psi} = -\psi_{xx} - 2\gamma|\psi|^2\psi, \tag{1}$$

under periodic boundary conditions, $\psi(-L, t) = \psi(L, t)$, for $t \in (0, T]$ with a final time $T > 0$, and with a prescribed initial condition, $\psi(x, 0)$ for $x \in (-L, L)$, where $\psi(x, t)$ denotes the complex-valued wave function. The NLSE (1) is completely integrable for $\gamma > 0$, i.e., there exists infinitely many integrals such as energy, momentum and norm [40, 38].

ALE [1] represents an integrable Hamiltonian semi-discretization of the NLSE (1) [24, 36, 38]

$$i\dot{\psi}_n = -\frac{1}{h^2}\left(\psi_{n+1} - 2\psi_n + \psi_{n-1}\right) - \gamma|\psi_n|^2\left(\psi_{n+1} + \psi_{n-1}\right) = 0, \tag{2}$$

with $h = 2L/N; \quad \psi_n = \psi(x_n, t); \quad x_n = -L + (n-1)h; \quad n = 1, \dots, N+1$. The solutions of the equation (2) converge to the solutions of the NLSE (1) when the step-size $h \to 0$. Under unitary time dependent transformation $\psi_n \to w_n e^{-2it/h^2}$, the ALE (2) can be written as a non-canonical Hamiltonian system [24, 38]

$$i\dot{w}_n = -\frac{1}{h^2}(w_{n+1} - w_{n-1})\left(1 + \gamma h^2|w_n|^2\right). \tag{3}$$

Separating the real and complex parts as $w = p + iq$, the equation (3) yields the coupled system

$$\dot{p}_n = -\frac{1}{h^2}\left(1 + \gamma h^2\left(p_n^2 + q_n^2\right)\right)(q_{n+1} + q_{n-1}),$$
$$\dot{q}_n = \frac{1}{h^2}\left(1 + \gamma h^2\left(p_n^2 + q_n^2\right)\right)(p_{n+1} + p_{n-1}). \tag{4}$$

Setting $\boldsymbol{p} = (p_1, \dots, p_N)^T$ and $\boldsymbol{q} = (q_1, \dots, q_N)^T$, the ALE (4) is given in matrix-vector form as the following non-canonical Hamiltonian system

$$\begin{pmatrix}\dot{\boldsymbol{p}} \\ \dot{\boldsymbol{q}}\end{pmatrix} = \begin{pmatrix} 0 & -M(\boldsymbol{p}, \boldsymbol{q}) \\ M(\boldsymbol{p}, \boldsymbol{q}) & 0 \end{pmatrix}\begin{pmatrix}\nabla_p H(\boldsymbol{p}, \boldsymbol{q}) \\ \nabla_q H(\boldsymbol{p}, \boldsymbol{q}),\end{pmatrix} \tag{5}$$

with the quadratic Hamiltonian $H(\boldsymbol{p}, \boldsymbol{q})$, and the matrix $M(\boldsymbol{p}, \boldsymbol{q})$ with nonlinear terms are given by

$$H(\boldsymbol{p}, \boldsymbol{q}) = \frac{1}{h^2}\sum_{n=1}^{N}\left(p_n p_{n-1} + q_n q_{n-1}\right), \quad M(\boldsymbol{p}, \boldsymbol{q}) = \text{diag}\left(m_1, \dots, m_N\right), \quad m_n = 1 + \gamma h^2\left(p_n^2 + q_n^2\right). \tag{6}$$

Under the above setting, the gradients of the Hamiltonian reduce to

$$\nabla_p H(\boldsymbol{p}, \boldsymbol{q}) = D\boldsymbol{p}, \quad \nabla_q H(\boldsymbol{p}, \boldsymbol{q}) = D\boldsymbol{q}, \quad D = \frac{1}{h^2}\begin{pmatrix} 0 & 1 & & & \\ 1 & 0 & 1 & & \\ & \ddots & \ddots & \ddots & \\ & & & 1 & 0 \end{pmatrix}. \tag{7}$$

Besides the Hamiltonian, there exist quadratic invariants, i.e., Casimirs, such as the momentum $\mathcal{I}$ whose discrete form is given by

$$I(\boldsymbol{p}, \boldsymbol{q}) = \sum_{n=1}^{N}\left(q_n\frac{p_{n+1} - p_{n-1}}{2h} - p_n\frac{q_{n+1} - q_{n-1}}{2h}\right). \tag{8}$$

For the solution vector $\boldsymbol{z} = (\boldsymbol{p}^T, \boldsymbol{q}^T)^T$, the ALE (5) is a $2N$-dimensional skew-gradient ODE of the form

$$\dot{\boldsymbol{z}} = S(\boldsymbol{z})\nabla_z H(\boldsymbol{z}), \tag{9}$$

where the skew-symmetric matrix $S(\boldsymbol{z})$ is given by

$$S(\boldsymbol{z}) = \begin{pmatrix} 0 & -M(\boldsymbol{p}, \boldsymbol{q}) \\ M(\boldsymbol{p}, \boldsymbol{q}) & 0 \end{pmatrix}.$$

Being a discrete gradient integrator, the AVF method given below, preserves the Hamiltonian (6) and the quadratic invariants such as the momentum (8), of the ALE (5) [16]

$$\frac{\boldsymbol{z}^{k+1} - \boldsymbol{z}^k}{\Delta t} = S\left(\frac{\boldsymbol{z}^{k+1} + \boldsymbol{z}^k}{2}\right) \int_0^1 \nabla_z H(\xi \boldsymbol{z}^{k+1} + (1-\xi)\boldsymbol{z}^k)d\xi, \quad k = 1, \ldots, K. \tag{10}$$

The AVF method is equivalent to the midpoint rule for quadratic Hamiltonians such as the ALE (5)

$$\frac{\boldsymbol{z}^{k+1} - \boldsymbol{z}^k}{\Delta t} = S\left(\frac{\boldsymbol{z}^{k+1} + \boldsymbol{z}^k}{2}\right) \nabla_z H\left(\frac{\boldsymbol{z}^{k+1} + \boldsymbol{z}^k}{2}\right), \quad k = 1, \ldots, K. \tag{11}$$

The damped NLSE

$$i\dot{\psi} = -\psi_{xx} - 2\gamma|\psi|^2\psi - i\mu\psi, \tag{12}$$

with the damping factor μ, describes resonant phenomena in nonlinear media, the nonlinear Faraday resonance in a vertically oscillating water and the effect of phase-sensitive amplifiers on solitons in optical fibers [19]. The Ablowitz-Ladik discretization of the damped NLSE (12) yields

$$\dot{p}_n = -\frac{1}{h^2}\left(1 + \gamma h^2 \left(p_n^2 + q_n^2\right)\right)(q_{n+1} + q_{n-1}) - \mu p_n,$$
$$\dot{q}_n = \frac{1}{h^2}\left(1 + \gamma h^2 \left(p_n^2 + q_n^2\right)\right)(p_{n+1} + p_{n-1}) - \mu q_n, \tag{13}$$

which represents a linearly perturbed non-canonical Hamiltonian system [30]. In matrix-vector form, the system (13) is a skew-gradient system with a damping term

$$\dot{\boldsymbol{z}} = S(\boldsymbol{z})\nabla_z H(\boldsymbol{z}) - \mu\boldsymbol{z}. \tag{14}$$

The energy or the Hamiltonian and the momentum dissipate like

$$\frac{d}{dt}\mathcal{I} = -\mu\mathcal{I} \implies \mathcal{I}(\boldsymbol{z}(t)) = e^{-\mu t}\mathcal{I}(\boldsymbol{z}^0).$$

Dissipation of the energy is expressed in form of the energy balance equation [30] given by

$$H(e^{X_1}Y_1) - H(e^{X_0}Y_0) = 0, \quad R_H = \ln\left(\frac{H(Y_1)}{H(Y_0)}\right) + \Delta t\mu. \tag{15}$$

Similarly, the dissipation of the momentum (8) is given as [30]

$$e^{2X_1}I(Y_1) - e^{2X_0}I(Y_0) = 0, \quad R_I = \ln\left(\frac{I(Y_1)}{I(Y_0)}\right) - 2\Delta t\mu. \tag{16}$$

The AVF method and the mid-point rule do not guarantee the correct rate of energy dissipation, i.e., the energy may be over or under damped [30]. The exponential mid-point rule preserves the correct dissipation rate of the energy and dissipative dynamics of the quadratic Casimirs such as the momentum and norm [30]. Approximation of the gradient of the Hamiltonian with

$$\bar{\nabla}H(e^{X_1}\boldsymbol{z}^{k+1}, e^{X_0}\boldsymbol{z}^k) = \int_0^1 \nabla H(\eta e^{X_1}\boldsymbol{z}^{k+1} + (1-\eta)e^{X_0}\boldsymbol{z}^k)d\eta, \tag{17}$$

yields the exponential midpoint rule [9, 30]

$$\frac{e^{X_1}\boldsymbol{z}^{k+1} - e^{X_0}\boldsymbol{z}^k}{\Delta t} = S\left(\frac{e^{X_1}\boldsymbol{z}^{k+1} + e^{X_0}\boldsymbol{z}^k}{2}\right)\bar{\nabla}H(e^{X_1}\boldsymbol{z}^{k+1}, e^{X_0}\boldsymbol{z}^k), \quad k = 1, \ldots, K, \tag{18}$$

where $X_\alpha = \mu(t_{k+\alpha} - t_{k+\frac{1}{2}})$. The exponential mid-point rule (18) preserves the dissipation rate of the invariants of the damped ALE (13)

$$\mathcal{I}^{k+1} = e^{-\mu\Delta t}\mathcal{I}^k, \quad k = 1, \ldots, K.$$

The midpoint rule (11) for the conservative ALE (5) and the exponential midpoint rule (18) for the dissipative ALE (13) are time-reversible, therefore second order convergent, and unconditionally stable time integrators.

3 Reduced-order modelling

The ROM for the damped ALE differs only by adding the linear damping term, therefore we describe the construction of the ROMs for the conservative ALE (5) whose compact form is given by (9).

3.1 POD reduced skew-gradient system

The low-dimensional ROMs are constructed by projecting the full-order system onto a low dimensional reduced space spanned by POD basis. The computation of the POD basis modes rely on a set of discrete solutions of the FOMs. To this end, let S_p and S_q denote the matrix of solution snapshots given by

$$\mathcal{S}_p = \begin{bmatrix} \boldsymbol{p}^1 \cdots \boldsymbol{p}^K \end{bmatrix} \in \mathbb{R}^{N \times K}, \qquad \mathcal{S}_q = \begin{bmatrix} \boldsymbol{q}^1 \cdots \boldsymbol{q}^K \end{bmatrix} \in \mathbb{R}^{N \times K},$$

where $\boldsymbol{p}^k, \boldsymbol{q}^k \in \mathbb{R}^N$, $k = 1, \ldots, K$, are the fully discrete solution vectors of the full-order ALE (5) through the mid-point rule (11). Then, the POD basis modes are taken as the left singular vectors related to the most dominant singular values from the singular value decomposition (SVD) of the snapshot matrices S_p and S_q

$$\mathcal{S}_p = W_p \Sigma_p Z_p^T \quad \mathcal{S}_q = W_q \Sigma_q Z_q^T,$$

where for $* \in \{p, q\}$, $W_* \in \mathbb{R}^{N \times K}$ and $Z_* \in \mathbb{R}^{K \times K}$ are orthonormal matrices whose column vectors are the left and right singular vectors, respectively, and $\Sigma_* \in \mathbb{R}^{K \times K}$ is the diagonal matrix containing the singular values $\sigma_{*,1} \geq \sigma_{*,2} \geq \cdots \geq \sigma_{*,K} \geq 0$. For some positive integer $N_r \ll \min\{N, K\}$, let $V_* \in \mathbb{R}^{N \times N_r}$ denotes the truncated matrix of POD modes consisting of the first N_r left singular vectors from W_*. For easy notation, we take the same number of POD modes for each component $* \in \{p, q\}$, but it can be taken different number of POD modes for either component p and q. The POD matrix V_* is the minimizer of the least squares error

$$\min_{V_* \in \mathbb{R}^{N \times N_r}} \|\mathsf{S}_* - V_* V_*^T \mathsf{S}_*\|_F^2 = \sum_{j=N_r+1}^{K} \sigma_{*,j}^2,$$

where $\| \cdot \|_F$ is the Frobenius norm. Once the POD modes are obtained, an approximation to the full-order solutions of (5) from the reduced space spanned by the POD modes, can be written as

$$\boldsymbol{p} \approx \widehat{\boldsymbol{p}} = V_p \boldsymbol{p}_r, \quad \boldsymbol{q} \approx \widehat{\boldsymbol{q}} = V_q \boldsymbol{q}_r, \tag{19}$$

where $\boldsymbol{p}_r, \boldsymbol{q}_r : [0, T] \mapsto \mathbb{R}^{N_r}$ are the coefficient vectors. The coefficient vectors are the solution of the $2N_r$-dimensional reduced system

$$\dot{\boldsymbol{z}}_r = V_z^T S(\widehat{\boldsymbol{z}}) \nabla_{\boldsymbol{z}} H(\widehat{\boldsymbol{z}}), \tag{20}$$

which is constructed by the Galerkin projection of the FOM (5) (or (9)) onto the reduced space. In the ROM (20), $\boldsymbol{z}_r = (\boldsymbol{p}_r^T, \boldsymbol{q}_r^T)^T : [0, T] \mapsto \mathbb{R}^{2N_r}$ is the vector of coefficients, $\widehat{\boldsymbol{z}} = V_z \boldsymbol{z}_r = (\widehat{\boldsymbol{p}}^T, \widehat{\boldsymbol{q}}^T)^T : [0, T] \mapsto \mathbb{R}^{2N}$ is the vector of reduced approximations, and the block diagonal matrix V_z contains the matrix of POD modes for each state variable

$$V_z = \begin{pmatrix} V_p & \\ & V_q \end{pmatrix} \in \mathbb{R}^{2N \times 2N_r}.$$

On the other hand, the reduced system (20) is not a skew-gradient system like the FOM (9). To recover a reduced skew-gradient system from the reduced system (20), we formally insert $V_z V_z^T \in \mathbb{R}^{2N \times 2N}$ between $S(\widehat{\boldsymbol{z}})$ and $\nabla_{\boldsymbol{z}} H(\widehat{\boldsymbol{z}})$ [20, 29]. This results in the POD reduced skew-gradient system

$$\dot{\boldsymbol{z}}_r = S_r(\boldsymbol{z}_r) \nabla_{\boldsymbol{z}_r} H(\boldsymbol{z}_r), \tag{21}$$

where $S_r(\boldsymbol{z}_r) = V_z^T S(V_z \boldsymbol{z}_r) V_z \in \mathbb{R}^{2N_r \times 2N_r}$ is the reduced skew-symmetric matrix and $\nabla_{\boldsymbol{z}_r} H(\boldsymbol{z}_r) = V_z^T \nabla_{\boldsymbol{z}} H(V_z \boldsymbol{z}_r) \in \mathbb{R}^{2N_r}$ is the reduced discrete gradient of the Hamiltonian. Then, the skew-gradient structure of the reduced system (21) yields

$$\frac{d}{dt} H(\widehat{\boldsymbol{z}}) = \frac{d}{dt} H(V_z \boldsymbol{z}_r) = \left[V_z^T \nabla_{\boldsymbol{z}} H(V_z \boldsymbol{z}_r) \right]^T \dot{\boldsymbol{z}}_r$$

$$= \left[\nabla_{\boldsymbol{z}_r} H(\boldsymbol{z}_r) \right]^T S_r(\boldsymbol{z}_r) \left[\nabla_{\boldsymbol{z}_r} H(\boldsymbol{z}_r) \right] = 0,$$

which means that the Hamiltonian $H(\widehat{\boldsymbol{z}})$ is preserved by the POD reduced skew-gradient system (21).

The approach that preserves the skew-symmetry of the reduced system (21) also preserves the energy dissipation property for dissipative systems such as the damped ALE [20]. Both the reduced systems are solved by the same time integrators as for the related FOMs, i.e., the POD reduced ALE (21) is solved in time with the implicit midpoint rule (11), whereas the POD reduced system of the dissipative ALE (14) is solved with the exponential midpoint rule (18).

3.2 POD-DEIM reduced skew-gradient system

The explicit form of the POD reduced skew-gradient system (21) reads as

$$
\begin{pmatrix} \dot{\boldsymbol{p}}_r \\ \dot{\boldsymbol{q}}_r \end{pmatrix} = \begin{pmatrix} 0 & -V_p^T M(V_z \boldsymbol{z}_r) V_q \\ V_q^T M(V_z \boldsymbol{z}_r) V_p & 0 \end{pmatrix} \begin{pmatrix} V_p^T \nabla_p H(V_z \boldsymbol{z}_r) \\ V_q^T \nabla_q H(V_z \boldsymbol{z}_r) \end{pmatrix},
\tag{22}
$$

where $M(V_z \boldsymbol{z}_r) = M(V_p \boldsymbol{p}_r, V_q \boldsymbol{q}_r) = M(\widehat{\boldsymbol{p}}, \widehat{\boldsymbol{q}})$ is given as in (6), i.e., $M(V_z \boldsymbol{z}_r) = \mathrm{diag}\,(m_1, \ldots, m_N)$ with $m_n = 1 + \gamma h^2 \left(\widehat{p}_i^2 + \widehat{q}_i^2 \right)$, $n = 1, \ldots, N$. Using the diagonal structure of the matrix $M(V_z \boldsymbol{z}_r)$, setting the nonlinear vector $\boldsymbol{m} = (m_1, \ldots, m_N)^T$, and inserting the discrete gradients of the Hamiltonian in (7), i.e., $\nabla_p H(\boldsymbol{z}) = D\boldsymbol{p}$ and $\nabla_q H(\boldsymbol{z}) = D\boldsymbol{q}$, the system (22) can be rewritten in the following explicit form

$$
\begin{aligned}
\dot{\boldsymbol{p}}_r &= -V_p^T \left[\boldsymbol{m} \odot (V_q V_q^T D V_q \boldsymbol{q}_r) \right], \\
\dot{\boldsymbol{q}}_r &= V_q^T \left[\boldsymbol{m} \odot (V_p V_p^T D V_p \boldsymbol{p}_r) \right],
\end{aligned}
\tag{23}
$$

with $\odot$ denoting the element-wise product of vectors. The POD reduced system (23) still depends on the dimension of the FOM, due to the nonlinear vector function $\boldsymbol{m} = (m_1, \ldots, m_N)^T : [0, T] \mapsto \mathbb{R}^N$. This can be circumvent applying the DEIM [17, 15]. The idea is to interpolate the nonlinear vector $\boldsymbol{m}$ using only $N_d \ll \min\{N, K\}$ entries. For this goal, one needs to compute the interpolation basis and an operator which selects the interpolation points and calculate the empirical basis. Let $\Phi = [\phi_1, \ldots, \phi_{N_d}] \in \mathbb{R}^{N \times N_d}$ denotes the N_d-dimensional interpolation basis. The interpolation basis $\{\phi_1, \ldots, \phi_{N_d}\}$ is constructed by applying the POD to the snapshot matrix S_m of the nonlinear vector, given by

$$
\mathsf{S}_m = [\boldsymbol{m}^1 \cdots \boldsymbol{m}^K] \in \mathbb{R}^{N \times K},
\tag{24}
$$

where $\boldsymbol{m}^k = \boldsymbol{m}(t_k)$ denotes the nonlinear vector computed by the fully discrete solutions of the FOM (5) at $t = t_k$. In other words, the DEIM basis modes $\phi_i \in \mathbb{R}^N$ are determined as the p left singular vectors related to the first N_d largest singular values from the SVD of the snapshot matrix S_m. Once the DEIM basis matrix Φ is obtained, the nonlinearity can be approximated as

$$
\boldsymbol{m}(t) \approx \Phi \mathsf{c}(t),
\tag{25}
$$

where $\mathsf{c}(t) : [0, T] \mapsto \mathbb{R}^{N_d}$ is the vector of time-dependent coefficients to be determined. In order to uniquely solve for the coefficient vector c, the overdetermined system (25) needs to be projected by multiplication from left by a matrix, say P, so that the product $\mathsf{P}^\top \Phi$ is invertible. The matrix P is indeed a selection matrix which is determined by a greedy algorithm based on the system residual [15]. Alternatively, the Q-DEIM [17] uses a different selection criteria for the sampling points than the original DEIM algorithm [15]. The Q-DEIM leads to better accuracy and stability properties of the computed selection matrix P using the pivoted QR-factorization of $\Phi^\top$. In the sequel, we use Q-DEIM for the calculation of the selection matrix P, see Algorithm 1.

Algorithm 1 Q-DEIM algorithm.

1: **Input:** Basis matrix $\Phi \in \mathbb{R}^{N \times p}$
2: **Output:** Selection matrix P
3: Perform pivoted QR factorization of $\Phi^\top$ so that $\Phi^\top \Pi = QR$
4: Set $\mathsf{P} = \Pi(:, 1:p)$

After computation of the selection matrix P, the coefficient vector $\mathsf{c}(t)$ is uniquely determined by solving the projected linear system $\mathsf{P}^\top \Phi \mathsf{c}(t) = \mathsf{P}^\top \boldsymbol{m}(t)$, by which the approximation (25) becomes

$$
\boldsymbol{m}(t) \approx \Psi \boldsymbol{m}_r(t),
\tag{26}
$$

where the matrix $\Psi := \Phi(\mathsf{P}^\top \Phi)^{-1} \in \mathbb{R}^{N \times N_d}$ is a constant matrix which can be precomputed in the offline stage. The reduced nonlinear vector $\boldsymbol{m}_r(t) := \mathsf{P}^\top \boldsymbol{m}(t) : [0, T] \mapsto \mathbb{R}^{N_d}$, is computed in the online stage with the reduced dimension $N_d \ll N$. In fact, the reduced nonlinear vector $\boldsymbol{m}_r(t)$ is nothing but N_d selected entries among the N entries of the nonlinear vector $\boldsymbol{m}$.

Inserting the DEIM approximation $\boldsymbol{m} \approx \Psi \boldsymbol{m}_r$ into the reduced system (23), we obtain the POD-DEIM reduced skew-gradient system

$$
\begin{aligned}
\dot{\boldsymbol{p}}_r &= -V_p^T \left[(\Psi \boldsymbol{m}_r) \odot (V_q V_q^T D V_q \boldsymbol{q}_r) \right], \\
\dot{\boldsymbol{q}}_r &= V_q^T \left[(\Psi \boldsymbol{m}_r) \odot (V_p V_p^T D V_p \boldsymbol{p}_r) \right].
\end{aligned}
\tag{27}
$$

3.3   The reduced quadratic system

The system (27) contains the precomputable constant matrices to be computed in the offline stage, and the reduced terms to be computed in the online stage, but they are still not separated. The precomputable constant matrices and the reduced terms can be separated by the use of tensor techniques, so that the solution of the POD-DEIM reduced skew-gradient system (27) is accelerated. We first rewrite the reduced system (27) in which Kronecker product $\otimes$ takes place of component-wise product $\odot$. This can be handled by using a selection matrix $G \in \mathbb{R}^{N \times N^2}$ satisfying the identity $G(\boldsymbol{a} \otimes \boldsymbol{b}) = \boldsymbol{a} \circ \boldsymbol{b}$ for any vectors $\boldsymbol{a}, \boldsymbol{b} \in \mathbb{R}^N$. The matrix G is generally called as a matricized tensor. Then, in terms of Kronecker product, the reduced system (27) yields

$$
\begin{aligned}
\dot{\boldsymbol{p}}_r &= -V_p^T G \left[(\Psi \boldsymbol{m}_r) \otimes (V_q V_q^T D V_q \boldsymbol{q}_r) \right], \\
\dot{\boldsymbol{q}}_r &= V_q^T G \left[(\Psi \boldsymbol{m}_r) \otimes (V_p V_p^T D V_p \boldsymbol{p}_r) \right].
\end{aligned}
\tag{28}
$$

Using the properties of Kronecker product, the system (28) further reduces to

$$
\begin{aligned}
\dot{\boldsymbol{p}}_r &= -V_p^T G \left(\Psi \otimes (V_q V_q^T D V_q) \right) (\boldsymbol{m}_r \otimes \boldsymbol{q}_r), \\
\dot{\boldsymbol{q}}_r &= V_q^T G \left(\Psi \otimes (V_p V_p^T D V_p) \right) (\boldsymbol{m}_r \otimes \boldsymbol{p}_r),
\end{aligned}
\tag{29}
$$

where it needs only the computation of the nonlinear vectors $\boldsymbol{m}_r \otimes \boldsymbol{p}_r : [0, T] \mapsto \mathbb{R}^{N_r N_d}$ and $\boldsymbol{m}_r \otimes \boldsymbol{q}_r : [0, T] \mapsto \mathbb{R}^{N_r N_d}$ in the online stage, and the terms $V_p^T G \left(\Psi \otimes (V_q V_q^T D V_q) \right) \in \mathbb{R}^{N_r \times (N_r N_d)}$ and $V_q^T G \left(\Psi \otimes (V_p V_p^T D V_p) \right) \in \mathbb{R}^{N_r \times (N_r N_d)}$ are constant matrices to be computed in the offline stage. By DEIM approximation with tensor setting, online computations scale with $\mathcal{O}(N_d N_r^2)$, whereas it scales with $\mathcal{O}(N_r N^2)$ if DEIM approximation is not used.

Apart from the computational efficiency in the online stage, we also follow a computationally efficient approach in the offline stage for the calculation of the constant matrices $G \left(\Psi \otimes (V_q V_q^T D V_q) \right) \in \mathbb{R}^{N \times (N_r N_d)}$ and $G \left(\Psi \otimes (V_p V_p^T D V_p) \right) \in \mathbb{R}^{N \times (N_r N_d)}$. Let us consider the calculation of the constant matrix $\widehat{G} := G \left(\Psi \otimes (V_q V_q^T D V_q) \right)$. Since it scales with the dimension of FOM, the explicit calculation of the matrix $\widehat{G}$ is inefficient. Using the structure of $\widehat{G}$, the matrix $\widehat{G}$ is given in MATLAB notation without constructing the matricized tensor G explicitly by

$$
\widehat{G} = \begin{pmatrix} \Psi(1,:) \otimes (V_q V_q^T D V_q)(1,:) \\ \vdots \\ \Psi(N,:) \otimes (V_q V_q^T D V_q)(N,:) \end{pmatrix}.
\tag{30}
$$

However, the computation in (30) needs N for loops in which a matrix product is done. This drawback can be overcome by the use of MULTIPROD [28] which handles multiple multiplications of the multi-dimensional arrays via virtual array expansion. More clearly, by the properties of Kronecker product, the ith row of the matrix $\widehat{G}$ in (30) is given equivalently by

$$
\widehat{G}(i,:) = (\text{vec}(\Psi(i,:)^\top (V_q V_q^T D V_q)(i,:))^\top, \quad i = 1, \ldots, N.
\tag{31}
$$

For each $i = 1, \ldots, N$, all the operations in (31) can be done at once by MULTIPROD as follows: we reshape the two-dimensional array (matrix) $\Psi \in \mathbb{R}^{N \times N_d}$ as a three-dimensional array $\widetilde{\Psi} \in \mathbb{R}^{N \times 1 \times N_d}$, and then we compute MULTIPROD of $(V_q V_q^T D V_q) \in \mathbb{R}^{N \times N_r \times 1}$ and $\widetilde{\Psi} \in \mathbb{R}^{N \times 1 \times N_d}$ in 2nd and 3th dimensions, which results in the three-dimensional array

$$
\widehat{\mathcal{G}} = \text{MULTIPROD}(V_q V_q^T D V_q, \widetilde{\Psi}) \in \mathbb{R}^{N \times N_r \times N_d},
\tag{32}
$$

where the tensor $\widehat{\mathcal{G}}$ collects all the matrix product of two matrices of sizes $N_r \times 1$ and $1 \times N_d$ within N iterations. Finally, the required matrix $\widehat{G} \in \mathbb{R}^{N \times (N_r N_d)}$ is obtained by reshaping the tensor $\widehat{\mathcal{G}}$ in (32) into a two-dimensional array of dimension $N \times (N_r N_d)$. Hence, utilizing the MULTIPROD, all the matrix products are done simultaneously in a single loop, which decreases the computational cost in the offline stage.

4   Numerical results

In this section, we illustrate the energy and momentum preserving properties for the conservative ALE and preservation of the dissipative structure of the damped ALE. The POD and DEIM basis are truncated according to the following relative cumulative energy criterion

$$
\min_{1 \leq p \leq K} \frac{\sum_{j=1}^{p} \sigma_j^2}{\sum_{j=1}^{K} \sigma_j^2} > 1 - \kappa,
\tag{33}
$$

where κ is a user-specified tolerance, and $p = N_r$ or $p = N_d$.

The accuracy of the ROMs is measured by the time averaged relative L_2-norm errors between FOM and ROM solutions

$$\|\boldsymbol{\psi} - \widehat{\boldsymbol{\psi}}\|_{rel} = \frac{1}{K} \sum_{k=1}^{K} \frac{\|\boldsymbol{\psi}^k - \widehat{\boldsymbol{\psi}}^k\|_{L^2}}{\|\boldsymbol{\psi}^k\|_{L^2}} \tag{34}$$

Conservation of the discrete invariants such as the energy (6) and momentum (8) of the conservative ALE (2) are measured using the time-averaged relative errors for the FOM and ROM

$$\|H\|_{\mathrm{abs}} = \frac{1}{K} \sum_{k=1}^{K} \frac{|H(\boldsymbol{w}^k) - H(\boldsymbol{w}^0)|}{|H(\boldsymbol{w}^0)|}, \quad \|I\|_{\mathrm{abs}} = \frac{1}{K} \sum_{k=1}^{K} \frac{|I(\boldsymbol{w}^k) - I(\boldsymbol{w}^0)|}{|I(\boldsymbol{w}^0)|}. \tag{35}$$

Similarly the dissipation rate of the discrete invariants such as the energy (15) and momentum (16) of the damped ALE (13) are measured using the time-averaged relative errors for the FOM and ROM

$$\|R_H\|_{\mathrm{abs}} = \frac{1}{K} \sum_{k=1}^{K} \frac{|R_H(\boldsymbol{w}^k) - R_H(\boldsymbol{w}^0)|}{|R_H(\boldsymbol{w}^0)|}, \quad \|R_I\|_{\mathrm{abs}} = \frac{1}{K} \sum_{k=1}^{K} \frac{|R_I(\boldsymbol{w}^k) - R_I(\boldsymbol{w}^0)|}{|R_I(\boldsymbol{w}^0)|}. \tag{36}$$

4.1   Conservative ALE

We consider the ALE (2) with soliton solution for $\gamma = 1$. The initial data is taken as [36]

$$\psi(x,0) = 2\eta e^{2i\xi x_n} sech(2\eta x_n),$$

where $x_n = -50 + 0.5(n-1), n = 1, \ldots N$, with $N = 200$, $h = 0.5$, $\eta = 0.05$, and $\xi = 0.5$. The time step is set as $\Delta t = 0.01$ for $0 < t \leq 50$. The snapshot matrices are computed by saving the full discrete solutions $\boldsymbol{p}$ and $\boldsymbol{q}$ at every five time steps, and they are of size 200×500. Figure 1 shows the normalized singular values, where normalized means that the first normalized singular value is one. The singular values of the snapshots corresponding to the state variables and to the nonlinear term decay slowly. The slow decay of the singular values is the characteristic for the problems with complex wave and transport phenomena [4, 31]. The rate of the decay of singular values is related to the Kolmogorov $r-$width which is a classical concept of nonlinear approximation theory as it describes the error arising from a projection onto the best-possible space of a given dimension r. It determines the linear reducibility of the underlying systems, which can be connected to the POD spectrum [33], therefore the selection of optimal number of POD/DEIM modes is important. By the use of much larger number of POD and DEIM modes, the conserved quantities in the reduced form are preserved, resulting accurate and stable solutions in long-term integration In our simulations, we set the tolerances $\kappa = 10^{-4}$ and $\kappa = 10^{-6}$ in (33), giving 21 POD and 21 DEIM modes. The relative FOM-ROM error (34) is 9.55e-03, whereas, the relative energy and momentum errors are 1.90e-04 and 2.29e-04, respectively.
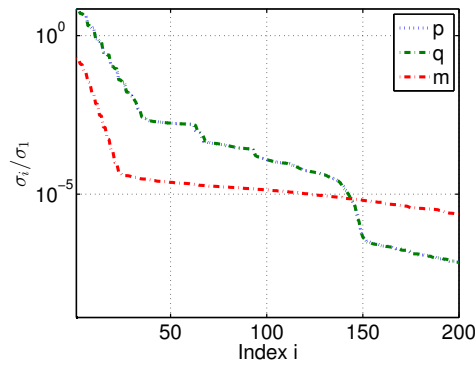
Figure 1: Decay of singular values for the states and the nonlinearity

In Figure 2 the Hamiltonian and momentum are preserved over the time without a drift, which ensures the stability of the solitons. In Table 1, the relative FOM-ROM errors (34) and time-averaged errors 35 of the invariants do not decrease much with increasing number of POD/DEIM modes. Therefore, the ROM solutions in Figure 3 accurately capture the full-order solutions.
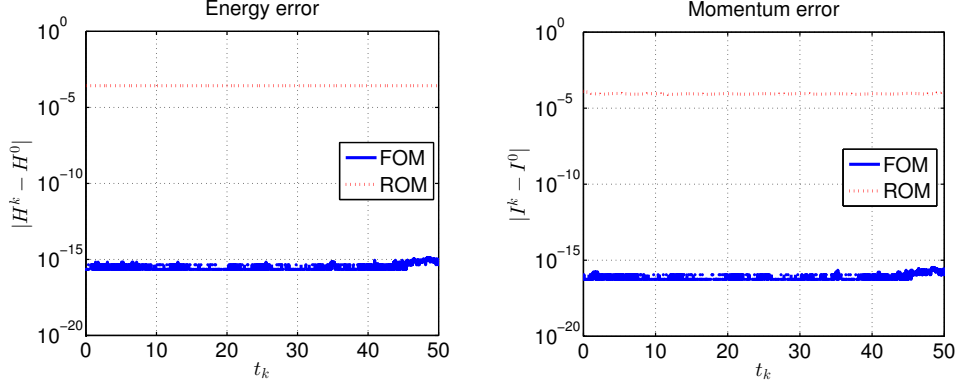
Figure 2: Preservation of the energy (left) and momentum (right)
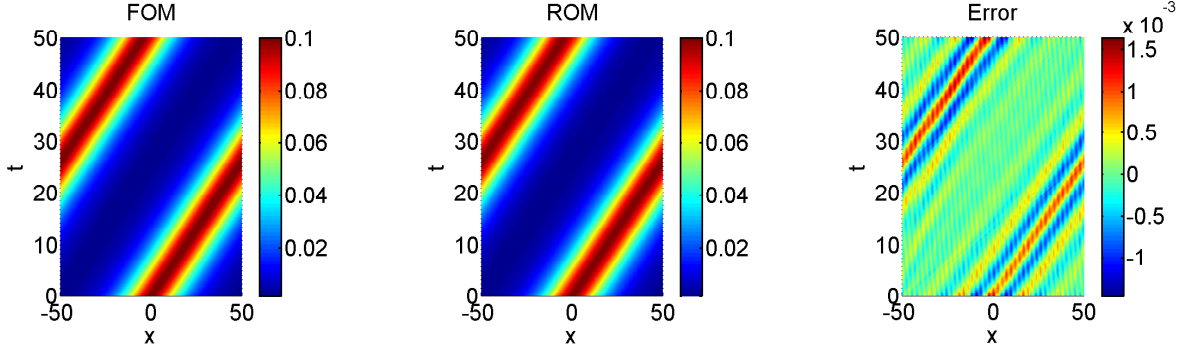
Figure 3: Solution profiles and error plot

Table 1: Time-averaged solution and energy/momentum errors

# POD/DEIM Modes	$\|\boldsymbol{\psi} - \widehat{\boldsymbol{\psi}}\|_{rel}$	$\|H\|_{abs}$	$\|I\|_{abs}$
20	1.06e-02	2.95e-04	2.95e-04
30	1.56e-03	4.82e-06	3.50e-06
40	1.73e-03	3.06e-07	3.29e-06
50	1.79e-03	2.21e-07	5.70e-06

4.2   Damped ALE

We consider the damped NLSE (12) with one soliton solution with $\gamma = 1$ and $\mu = 0.01$ [19]. The solutions are computed with a time step $\Delta t = 0.01$ in the time interval $t \in [0, 60]$, and on the spatial domain $x \in [-64, 64]$ with the mesh size $h = 0.25$. The resulting ALE is of size $N = 512$. The Initial condition is taken as

$$\psi(x, 0) = \frac{\sqrt{2}}{2} \exp\left(i \frac{x + p}{2}\right) \operatorname{sech}\left(\frac{x + p}{2}\right),$$

with the initial phase $p = 20$. The full order solutions are saved at every five time steps, for which the snapshot matrices are of size 512×300.

In Figure 4, singular values of the snapshots for the damped ALE show a similar decay behavior as for the conservative ALE. The number of the POD and DEIM modes are calculated as $N_r = 40$ and $N_d = 49$, corresponding to the tolerances $\kappa = 10^{-5}$ and $\kappa = 10^{-7}$, respectively. In order to fulfill the energy and momentum balance in Figures 5-6, the tolerances are taken as one order smaller than for the conservative ALE. The relative FOM-ROM error (34) is 7.22e-03.

Setting the tolerances $\kappa = 10^{-4}$ and $\kappa = 10^{-7}$ in (33), results in $N_r = 40$ and $N_d = 49$ POD and DEIM modes, respectively. The relative FOM-ROM error (34) is 7.09e-03, whereas the relative energy and momentum balance

9
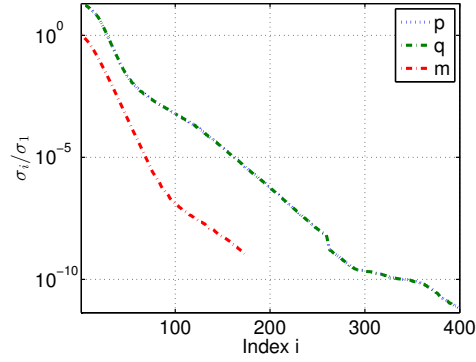
Figure 4: Decay of singular values for the states and the nonlinearity
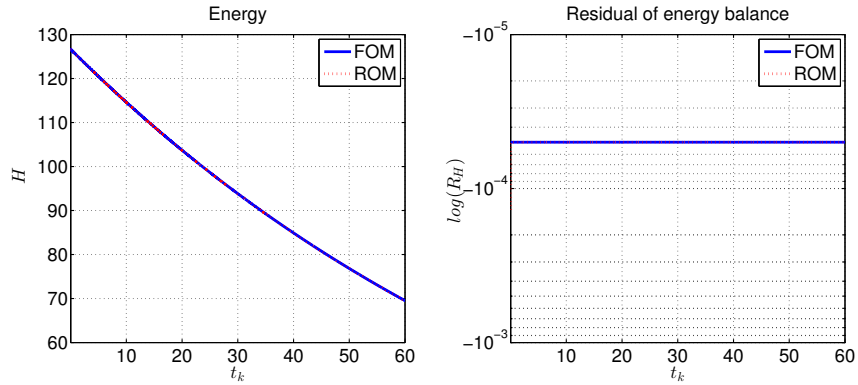
Figure 5: Energy (left) and residual of energy balance (right)
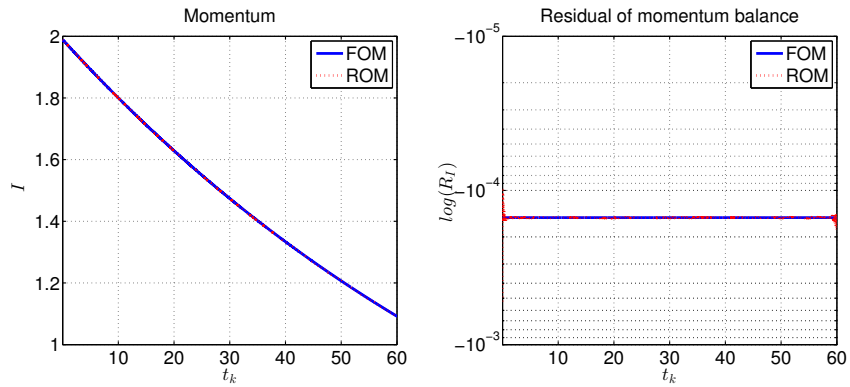
Figure 6: Momentum (left) and residual of momentum balance (right)

errors (36) are 1.38-04 and 5.24e-04, respectively. The solution error and residuals of the energy/momentum balances are saturated around 50 POD/DEIM modes in Table 2, similar to the conservative ALE in Figure 1. The FOM/ROM solutions in Figure 7 are almost identical, and the energy and momentum dissipate with correct rates in Figures 5-6.
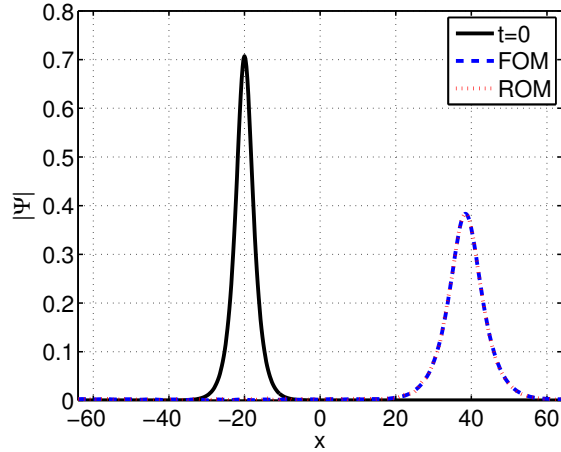
Figure 7: Initial soliton and soliton solutions at final time

Table 2: Time-averaged solution and energy/momentum balance errors

# POD/DEIM Modes	$\|\boldsymbol{\psi} - \widehat{\boldsymbol{\psi}}\|_{rel}$	$\|R_H\|_{\text{abs}}$	$\|R_I\|_{\text{abs}}$
20	2.24e-01	9.64e-02	1.95e-01
30	3.89e-02	3.19e-03	8.55e-03
40	7.07e-03	1.38e-04	5.25e-04
50	1.70e-03	5.39e-05	1.65e-04
60	7.23e-04	5.04e-05	1.51e-04

5   Conclusions

In this paper, structure-preserving ROMs are constructed for the conservative and dissipative ALEs. The reduced system can be identified by accurately preserved reduced energy and momentum for the conservative and dissipative ALEs in long time integration, that mimics those of the high-fidelity system and ensures the stability and robustness of the reduced-order soliton solutions. Relatively large number of POD and DEIM modes show the limitation of the linear MOR techniques such as POD and DEIM for problems associated with transport and wave type phenomena as in this paper. The nonlinear model order reduction on manifolds [11] or kernel methods [18] can produce accurate solutions in low dimensional reduced spaces, which will be subject of future research.

References

[1] M. J. Ablowitz and J. F. Ladik. A nonlinear difference scheme and inverse scattering. *Studies in Applied Mathematics*, 55(3):213–229, 1976.

[2] B. M. Afkham and J. S. Hesthaven. Structure-preserving model-reduction of dissipative Hamiltonian systems. *Journal of Scientific Computing*, 81(1):3–21, 2019.

[3] B. M. Afkham and J.S. Hesthaven. Structure preserving model reduction of parametric Hamiltonian systems. *SIAM Journal on Scientific Computing*, 39(6):A2616–A2644, 2017.

[4] S. E. Ahmed and O. San. Breaking the Kolmogorov barrier in model reduction of fluid flows. *Fluids*, 5(1), 2020.

[5] P. Benner and P. Goyal. Interpolation-based model order reduction for polynomial systems. *SIAM Journal on Scientific Computing*, 43(1):A84–A108, 2021.

[6] P. Benner, P. Goyal, and S. Gugercin. $\langle_2$-quasi-optimal model order reduction for quadratic-bilinear control systems. *SIAM Journal on Matrix Analysis and Applications*, 39(2):983–1032, 2018.

[7] P. Benner, S. Grivet-Talocia, A. Quarteroni, G. Rozza, W. Schilders, and M.L. Silveira. *Model Order Reduction: Volume 2: Snapshot-Based Methods and Algorithms*. De Gruyter, 2020.

[8] G Berkooz, P Holmes, and J L Lumley. The proper orthogonal decomposition in the analysis of turbulent flows. *Annual Review of Fluid Mechanics*, 25(1):539–575, 1993.

[9] A. Bhatt, D. Floyd, and B. E. Moore. Second order conformal symplectic schemes for damped Hamiltonian systems. *Journal of Scientific Computing*, 66(3):1234–1259, 2016.

[10] P. Buchfink, A. Bhatt, and B. Haasdonk. Symplectic model order reduction with non-orthonormal bases. *Mathematical & Computational Applications*, 24(2):Paper No. 43, 26, 2019.

[11] P. Buchfink, S. Glas, and B. Haasdonk. Symplectic model reduction of Hamiltonian systems on nonlinear manifolds, 2021.

[12] P. Buchfink, B. Haasdonk, and S. Rave. Psd-greedy basis generation for structure-preserving model order reduction of Hamiltonian systems. *Proceedings of the Conference Algoritmy*, pages 151–160, 2020.

[13] K. Carlberg, R. Tuminaro, and P. Boggs. Preserving Lagrangian structure in nonlinear model reduction with application to structural dynamics. *SIAM J. Sci. Comput.*, 37(2):B153–B184, 2015.

[14] S. Chaturantabut, C. Beattie, and S. Gugercin. Structure-preserving model reduction for nonlinear port-Hamiltonian systems. *SIAM Journal on Scientific Computing*, 38(5):B837–B865, 2016.

[15] S. Chaturantabut and D. C. Sorensen. Nonlinear model reduction via discrete empirical interpolation. *SIAM J. Sci. Comput.*, 32(5):2737–2764, 2010.

[16] D. Cohen and E. Hairer. Linear energy-preserving integrators for Poisson systems. *BIT Numerical Mathematics*, 51(1):91–101, 2011.

[17] Z. Drmač and S. Gugercin. A new selection operator for the discrete empirical interpolation method–improved a priori error bound and extensions. *SIAM Journal on Scientific Computing*, 38(2):A631–A648, 2016.

[18] P. Díez, A. Muixí, S. Zlotnik, and A. García-González. Nonlinear dimensionality reduction for parametric problems: A kernel proper orthogonal decomposition. *International Journal for Numerical Methods in Engineering*, 122(24):7306–7327, 2021.

[19] H. Fu, W.E. Zhou, X. Qian, S.H. Song, and L.Y. Zhang. Conformal structure-preserving method for damped nonlinear Schrödinger equation. *Chinese Physics B*, 25(11):110201, 2016.

[20] Y. Gong, Q. Wang, and . Wang. Structure-preserving Galerkin POD reduced-order modeling of Hamiltonian systems. *Computer Methods in Applied Mechanics and Engineering*, 315:780 – 798, 2017.

[21] J. S. Hesthaven, C. Pagliantini, and G. Rozza. Reduced basis methods for time-dependent problems. *Acta Numerica*, 31:265–345, 2022.

[22] Jan S. Hesthaven and Cecilia Pagliantini. Structure-preserving reduced basis methods for Poisson systems. *Mathematics of Computation*, 90(330):1701–1740, 2021.

[23] Jan S. Hesthaven, Cecilia Pagliantini, and Nicolò Ripamonti. Rank-adaptive structure-preserving model order reduction of Hamiltonian systems. *ESAIM. Mathematical Modelling and Numerical Analysis*, 56(2):617–650, 2022.

[24] A.L. Islas, D.A. Karpeev, and C.M. Schober. Geometric integrators for the nonlinear Schrödinger equation. *Journal of Computational Physics*, 173(1):116 – 148, 2001.

[25] B. Karasözen and M. Uzunca. Energy preserving model order reduction of the nonlinear Schrödinger equation. *Advances in Computational Mathematics*, 44(6):1769–1796, 2018.

[26] B. Karasözen, S. Yıldız, and M. Uzunca. Structure preserving model order reduction of shallow water equations. *Mathematical Methods in the Applied Sciences*, 44(1):476–492, 2021.

[27] B. Karasøzen, S. Yıldız, and M. Uzunca. Energy preserving reduced-order modeling of the rotating thermal shallow water equation. *Physics of Fluids*, 34(5):056603, 2022.

[28] P. d. Leva. MULTIPROD TOOLBOX, multiple matrix multiplications, with array expansion enabled. Technical report, University of Rome Foro Italico, Rome, 2008.

[29] Y. Miyatake. Structure-preserving model reduction for dynamical systems with a first integral. *Japan Journal of Industrial and Applied Mathematics*, 36(3):1021–1037, 2019.

[30] B. E. Moore. Exponential integrators based on discrete gradients for linearly damped/driven Poisson systems. *Journal of Scientific Computing*, 87(2):Paper No. 56, 18, 2021.

[31] M. Ohlberger and S. Rave. Reduced basis methods: Success, limitations and future challenges. *Proceedings of the Conference Algoritmy*, pages 1–12, 2016.

[32] C. Pagliantini. Dynamical reduced basis methods for Hamiltonian systems. *Numerische Mathematik*, 148(2):409–448, 2021.

[33] B. Peherstorfer. Breaking the Kolmogorov barrier with nonlinear model reduction. *Notices of the American Mathematical Society*, 65(9):725–733, 2022.

[34] L. Peng and K. Mohseni. Geometric model reduction of forced and dissipative hamiltonian systems. In *2016 IEEE 55th Conference on Decision and Control (CDC)*, pages 7465–7470, 2016.

[35] L. Peng and K. Mohseni. Symplectic model reduction of Hamiltonian systems. *SIAM Journal on Scientific Computing*, 38(1):A1–A27, 2016.

[36] C. M. Schober. Symplectic integrators for the Ablowitz-Ladik discrete nonlinear Schrödinger equation. *Physics Letters. A*, 259(2):140–151, 1999.

[37] L. Sirovich. Turbulence and the dynamics of coherent structures. III. Dynamics and scaling. *Quart. Appl. Math.*, 45(3):583–590, 1987.

[38] Y. Tang, J. Cao, X. Liu, and Y. Sun. Symplectic methods for the Ablowitz–Ladik discrete nonlinear Schrödinger equation. *Journal of Physics A: Mathematical and Theoretical*, 40(10):2425–2437, 2007.

[39] M. Uzunca, B. Karasözen, and S. Yıldız. Structure-preserving reduced-order modeling of Korteweg–de Vries equation. *Mathematics and Computers in Simulation*, 188:193–211, 2021.

[40] V. E. Zaharov and S. V. Manakov. The complete integrability of the nonlinear Schrödinger equation. *Theoretical and Mathematical Physics*, 19:332–343, 1974.